Inorg. Chem. **2009**, *48*, 1638−1648

Ligands for Dinitrogen Fixation at Schrock-Type Catalysts

Stephan Schenk and Markus Reiher*

Laboratorium für Physikalische Chemie, ETH Zürich, Wolfgang-Pauli-Str. 10, CH-8093 Zürich, Switzerland

Received October 23, 2008

Catalytic dinitrogen reduction with the Schrock complex is still hampered by low turn-over numbers that are likely to result from a degradation of the chelate ligand. In this work, we investigate modifications of the original $HIPTN_3N$ ligand applied by Schrock and co-workers in catalytic reduction of dinitrogen with density functional methods. We focus on ligands that are substituted in the *para* position of the central phenyl ring of the terphenyl moieties and on a ligand where the bridging nitrogen is exchanged by phosphorus. In addition, results for tris(pyrrolyl-α-methyl)amine, tris(pyrrolyl-α-ethyl)amine, and tris[2-(3-xylyl-imidazol-2-ylidene)ethyl]amine are reported. For this study, we take into account the full ligands without approximating them by model systems. Reaction energies for the various derivatives of $HIPTN_3N$ are found to be similar to those of the unchanged parent system. However, the most promising results for catalysis are obtained for the [{tris[2-(3-xylyl-imidazol-2-ylidene)ethyl]amine}Mo](N_2) complex. Feasibility of the exchange of NH_3 by N_2 is found to be the pivotal question whether a complex can become a potential catalyst or not. A structure−reactivity relationship is derived which allows for the convenient estimation of the reaction energy for the NH_3/N_2 exchange reaction solely from the wavenumber of the N≡N stretching vibration. This relationship may guide experiments as soon as a dinitrogen Mo complex is formed.

1. Introduction

The catalytic reduction of dinitrogen to ammonia under ambient conditions was developed by Yandulov and Schrock[1,2] for a molybdenum catalyst with a substituted trisethylenetetramine ligand (Scheme 1, left). The ligand applied in these studies features hexa-*iso*-propyl terphenyl substituents (HIPT) and is usually abbreviated as $HIPTN_3N$. The five-coordinated Schrock molybdenum complex is very well suited and especially designed for dinitrogen reduction. Nevertheless, the small turnover number of four[1] demands improvement. It is likely that the ligand degrades in the protonation/reduction steps.[3]

In previous work, we investigated mechanistic details of the catalytic N_2 reduction facilitated by [($HIPTN_3N$)Mo(N_2)] (see also Supporting Information, Figure S1) with density functional methods.[3,4] Quantum chemical studies on smaller model complexes have also been carried out.[5−9] The calculated results are in remarkable agreement with experiment.[10] Given this validity of the computational approach, we may take the next step and investigate modified ligands to eventually identify those which are more stable but still facilitate dinitrogen reduction. However, the rigid structure of the latter does not allow for many modifications, and we consider those studied in this work as prototypical.

In the present work, as a first step toward identification of a more efficient catalyst, we will investigate the range of changes in the reaction thermodynamics upon variation of the chelate ligand under the boundary condition that the principal tetradentate structure of the ligand is kept. We choose several ligands that have been derived from the parent $HIPTN_3N$ structure (Scheme 1, left). We focus on ligands

* To whom correspondence should be addressed. E-mail: markus.reiher@phys.chem.ethz.ch.

(1) Yandulov, D. V.; Schrock, R. R. *Science* **2003**, *301*, 76–78.
(2) Yandulov, D. V.; Schrock, R. R. *J. Am. Chem. Soc.* **2002**, *124*, 6252–6253.
(3) Schenk, S.; Le Guennic, B.; Kirchner, B.; Reiher, M. *Inorg. Chem.* **2008**, *47*, 3634–3650; erratum: *Inorg. Chem.* **2008**, *47*, 7934.
(4) Reiher, M.; Le Guennic, B.; Kirchner, B. *Inorg. Chem.* **2005**, *44*, 9640–9642.
(5) Le Guennic, B.; Kirchner, B.; Reiher, M. *Chem.—Eur. J.* **2005**, *11*, 7448–7460.
(6) Khoroshun, D. V.; Musaev, D. G.; Morokuma, K. *Mol. Phys.* **2002**, *100*, 523–532.
(7) Cao, Z.; Zhou, Z.; Wan, H.; Zhang, Q. *Int. J. Quantum Chem.* **2005**, *103*, 344–353.
(8) Studt, F.; Tuczek, F. *Angew. Chem., Int. Ed.* **2005**, *44*, 5639–5642; *Angew. Chem.* **2005**, *117*, 5783−5787.
(9) Magistrato, A.; Robertazzi, A.; Carloni, P. *J. Chem. Theory Comput.* **2007**, *3*, 1708–1720.
(10) Schrock, R. R. *Angew. Chem., Int. Ed.* **2008**, *47*, 5512–5522; *Angew. Chem.* **2008**, *120*, 5594−5605.

10.1021/ic802037w CCC: $40.75
Published on Web 01/12/2009

where the central phenyl ring of the terphenyl groups is substituted at the *para* position,[11] the *iso*-propyl groups are replaced by *tert*-butyl,[11] and on those where the bridging amine nitrogen has been exchanged by a phosphorus atom as suggested by Schrock.[12] In addition, we will also discuss a recently proposed tris(pyrrolyl-α-methyl)amine,[13] as well as the corresponding tris(pyrrolyl-α-ethyl)amine ligand (Scheme 1, center). Furthermore, investigations on the tris[2-(3-xylyl-imidazol-2-ylidene)ethyl]amine[14] ligand (Scheme 1, right) are reported.

Reduction of steric congestion at the metal center by replacement of only one of the terphenyl moieties in $HIPTN_3N$ by smaller groups (so-called hybrid ligands) results in a complete loss of the desired catalytic activity because of a hydrogenase shunt.[15] The ligands derived from $HIPTN_3N$ investigated herein barely change the shielding of the active site (except for **htbt** which increases the shielding), and we therefore believe that they will not suffer from increased hydrogenase activity. However, we cannot exclude that unforeseen side reactions may render a catalytic reduction of dinitrogen impossible. This is especially true for the three non-HIPT derived ligands for which no investigation of their potential to afford catalysis has been reported up to now. Albeit *N*-heterocyclic carbenes are generally known to be mere spectator ligands, there are some reports that show that this is not necessarily always true[16−25] Therefore, the thermodynamic feasibility of the catalytic cycle with a particular ligand addressed in this paper is a necessary but not necessarily sufficient requirement for a successful catalyst.

This work is organized as follows: We first describe how we define the reaction energies. This is followed by a detailed discussion of the catalytic capabilities of the individual ligands. At the end, parameters characterizing an efficient catalyst are deduced.

2. Results and Discussion

2.1. Definition of Reaction Energies. For the comparison of different ligands, we concentrate on net reactions for the transfer of one electron and one proton onto a N_xH_y moiety,

$$[\mathbf{Mo}](N_xH_y) + HA + Red \rightarrow [\mathbf{Mo}](N_xH_{y+1}) + A^- + Red^+ \quad (1)$$

where [**Mo**] is a short-hand notation for the complex of the corresponding ligand with molybdenum whereas HA denotes the acid and Red the electron source. Naturally, the reaction energy does not depend on whether the electron or the proton is transferred first. We therefore will not provide detailed information for the elementary steps, that is, protonation/reduction of [**Mo**](N_xH_y) as discussed in extenso in ref 3, but focus on the overall electronic energy change associated with reaction 1.

Following the same approach as in ref 3, reaction 1 can be split into the following steps:

$$[\mathbf{Mo}](N_xH_y) + H^+ + e^- \rightarrow [\mathbf{Mo}](N_xH_{y+1}) \quad (2)$$

$$HA \rightarrow A^- + H^+ \quad (3)$$

$$Red \rightarrow Red^+ + e^- \quad (4)$$

where the charge combinations or separations lead to at first sight unphysically large reaction energies. The absolute values of these energies would be quenched in a dielectric continuum, but we refrain from introducing such continuum solvation models for reasons discussed in detail in ref 3. The overall electronic energy change for reaction 1, $\Delta_R E^{net}$, is given by

$$\Delta_R E^{net} = \Delta_R E^{(2)} + \Delta_R E^{(3)} + \Delta_R E^{(4)} \quad (5)$$

$$= \Delta_R E^{intrinsic} - PA - EA \quad (6)$$

where $\Delta_R E^{(n)}$ denotes the reaction energy for reaction (n), PA the intrinsic proton affinity of the corresponding base A^-, and EA the intrinsic electron affinity of the oxidized reductant Red^+.

We report $\Delta_R E^{intrinsic}$ values in Table 1. Reaction energies for a particular set of reactants can be calculated with the corresponding PA and EA values given in ref 3. For convenience, we also list the reaction energies obtained with 2,6-dimethyl pyridinium (lutidinium) and decamethyl chromocene, $Cr(cp^*)_2$, in Table 2.

For an assessment of the different ligands, we compare the corresponding reaction energies with those obtained for the **hipt** ligand. Naturally, these differences are not affected by the particular choice of reductant and/or acid employed. The EA and PA values, respectively, merely shift all reaction energies by a constant value; the *difference* of two reaction energies thus remains unchanged.

2.2. Catalytic Capabilities of Individual Ligands. 2.2.1. hipt_oh and hipt_br. The data in Table 3 show that introduction of an OH (**hipt_oh**) or Br group (**hipt_br**) at the *para* position of the central phenyl ring of the terphenyl moieties leads to small changes in the reaction energies no larger than 10 kJ mol^{-1}. Although this modulation of the reaction energies

(11) Ritleng, V.; Yandulov, D. V.; Weare, W. W.; Schrock, R. R.; Hock, A. S.; Davis, W. M. *J. Am. Chem. Soc.* **2004**, *126*, 6150–6163.
(12) Schrock, R. R.; 2007;private communication.
(13) Wampler, K. M.; Schrock, R. R. *Inorg. Chem.* **2007**, *46*, 8463–8465.
(14) Hu, X.; Meyer, K. *J. Organomet. Chem.* **2005**, *690*, 5474–5484.
(15) Weare, W. W.; Schrock, R. R.; Hock, A. S.; Müller, P. *Inorg. Chem.* **2006**, *45*, 9185–9196.
(16) Danopoulos, A. A.; Pugh, D.; Wright, J. A. *Angew. Chem., Int. Ed.* **2008**, *47*, 9765–9767; *Angew. Chem.* **2008**, *120*, 9911−9913.
(17) Pugh, D.; Boyle, A.; Danopoulos, A. A. *Dalton Trans.* **2008**, 1087–1094.
(18) Becker, E.; Stingl, V.; Dazinger, G.; Mereiter, K.; Kirchner, K. *Organometallics* **2007**, *26*, 1531–1535.
(19) Waltman, A. W.; Ritter, T.; Grubbs, R. H. *Organometallics* **2006**, *25*, 4238–4239.
(20) Corberán, R.; Sanaú, M.; Peris, E. *Organometallics* **2006**, *25*, 4002–4008.
(21) Galan, B. R.; Gembicky, M.; Dominiak, P. M.; Keister, J. B.; Diver, S. T. *J. Am. Chem. Soc.* **2005**, *127*, 15702–15703.
(22) Scott, N. M.; Dorta, R.; Stevens, E. D.; Correa, A.; Cavallo, L.; Nolan, S. P. *J. Am. Chem. Soc.* **2005**, *127*, 3516–3526.
(23) Danopoulos, A. A.; Tsoureas, N.; Green, J. C.; Hursthouse, M. B. *Chem. Commun.* **2003**, 756–757.
(24) Jazzar, R. F. R.; Macgregor, S. A.; Mahon, M. F.; Richards, S. P.; Whittlesey, M. K. *J. Am. Chem. Soc.* **2002**, *124*, 4944–4945.
(25) McGuinness, D. S.; Cavell, K. J.; Yates, B. F.; Skelton, B. W.; White, A. H. *J. Am. Chem. Soc.* **2001**, *123*, 8317–8328.

Scheme 1. Schematical Drawing of Different Complexes That Have Already Been Experimentally Investigated (**hipt**, **hipt_br**, and **htbt**) or Suggested (**hipt_oh**, **hipt_p**, and **tpa_me**) As Catalysts for Reduction of Dinitrogen

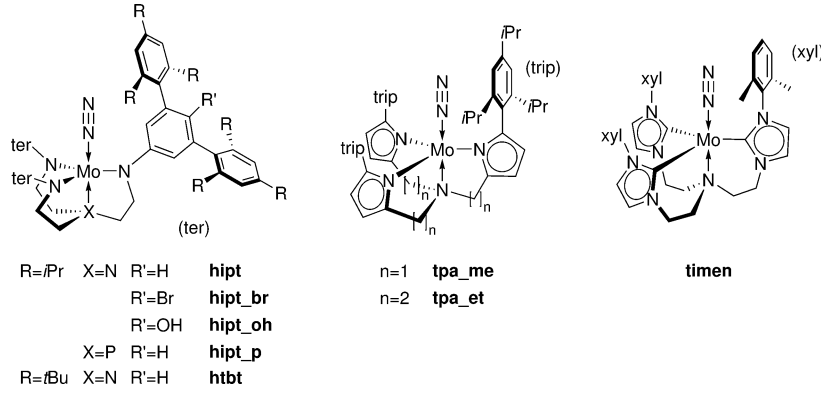

Table 1. Intrinsic Reaction Energies $\Delta_R E^{intrinsic}$ (kJ mol^{-1}) for Reaction 2 with Different Ligands

educt	product(s)	**hipt**	**hipt_oh**	**hipt_br**	**hipt_p**	**htbt**	**tpa_me**	**tpa_et**	**timen(3)**	**timen(0)**
[**Mo**](N$_2$)	[**Mo**](NNH)	−1548.3	−1551.2	−1552.5	−1525.4	−1552.4	−1552.9	−1548.3	−1567.3	−1500.8
[**Mo**](NNH)	[**Mo**](NNH$_2$)	−1486.0	−1485.5	−1488.9	−1501.1	−1488.5	−1529.9	−1519.5	−1599.6	−1552.5
[**Mo**](NNH$_2$)	[**Mo**](N) + NH$_3$	−1688.5	−1684.6	−1681.8	−1630.2	−1696.2	−1623.5	−1667.1	−1520.7	−1676.1
[**Mo**](N)	[**Mo**](NH)	−1493.6	−1494.8	−1497.0	−1554.3	−1499.2	−1560.4	−1526.3	−1615.8	−1547.2
[**Mo**](NH)	[**Mo**](NH$_2$)	−1589.3	−1587.0	−1589.4	−1593.7	−1582.6	−1558.3	−1579.2	−1557.9	−1520.6
[**Mo**](NH$_2$)	[**Mo**](NH$_3$)	−1554.7	−1546.9	−1548.6	−1591.6	−1549.8	−1580.7	−1597.7	−1619.0	−1492.3

Table 2. Net Reaction Energies $\Delta_R E^{net}$ (kJ mol^{-1}) for Reaction 1 with Lutidinium As Proton and Cr(cp*)$_2$ As Electron Source[a]

educt	product(s)	**hipt**	**hipt_oh**	**hipt_br**	**hipt_p**	**htbt**	**tpa_me**	**tpa_et**	**timen(3)**	**timen(0)**
[**Mo**](N$_2$)	[**Mo**](NNH)	−63.0	−65.9	−67.2	−40.2	−67.1	−67.7	−63.1	−82.0	−15.5
[**Mo**](NNH)	[**Mo**](NNH$_2$)	−0.7	−0.2	−3.6	−15.9	−3.2	−44.6	−34.2	−114.4	−67.2
[**Mo**](NNH$_2$)	[**Mo**](N) + NH$_3$	−203.2	−199.3	−196.5	−144.9	−210.9	−138.2	−181.8	−35.4	−190.8
[**Mo**](N)	[**Mo**](NH)	−8.3	−9.5	−11.7	−69.0	−13.9	−75.1	−41.0	−130.5	−62.0
[**Mo**](NH)	[**Mo**](NH$_2$)	−104.0	−101.7	−104.2	−108.5	−97.3	−73.0	−94.0	−72.6	−35.3
[**Mo**](NH$_2$)	[**Mo**](NH$_3$)	−69.4	−61.6	−63.4	−106.4	−64.5	−95.4	−112.4	−133.7	−7.0
[**Mo**](NH$_3$)	[**Mo**](N$_2$)	−40.5	−50.9	−42.6	−4.5	−32.2	+4.9	+37.3	+79.4	−111.4

[a] Additionally, the reaction energy for the NH$_3$/N$_2$ exchange is given. The energies were calculated according to equation 6 with PA/EA values from ref 3.

Table 3. Differences in Reaction Energies (kJ mol^{-1}) for Reaction 1 Obtained with Different Ligands Given with Respect to the Results for the **hipt** Complex

educt	product(s)	**hipt_oh**	**hipt_br**	**hipt_p**	**htbt**	**tpa_me**	**tpa_et**	**timen(3)**	**timen(0)**
[**Mo**](N$_2$)	[**Mo**](NNH)	−2.9	−4.2	+22.9	−4.1	−4.6	0.0	−19.0	+47.5
[**Mo**](NNH)	[**Mo**](NNH$_2$)	+0.5	−2.9	−15.1	−2.5	−43.9	−33.5	−113.6	−66.5
[**Mo**](NNH$_2$)	[**Mo**](N) + NH$_3$	+3.9	+6.7	+58.3	−7.7	+65.0	+21.4	+167.8	+12.4
[**Mo**](N)	[**Mo**](NH)	−1.2	−3.4	−60.7	−5.6	−66.8	−32.7	−122.2	−53.6
[**Mo**](NH)	[**Mo**](NH$_2$)	+2.3	−0.1	−4.4	+6.7	+31.0	+10.1	+31.4	+68.7
[**Mo**](NH$_2$)	[**Mo**](NH$_3$)	+7.8	+6.1	−36.9	+4.9	−26.0	−43.0	−64.3	+62.4
[**Mo**](NH$_3$)	[**Mo**](N$_2$)	−10.4	−2.1	+36.0	+8.3	+45.4	+77.8	+119.9	−70.9

is small, it is still remarkable in view of the fact that the substitution of H by OH or Br, respectively, was made comparatively far away from the reaction center (one might argue in favor of an electronic coupling from the OH group in *para* position of the phenyl substituent at the amide N to the Mo center). Complexes with both ligands, **hipt_oh** and **hipt_br**, should show catalytic activity comparable to the parent [(**hipt**)-Mo] system. For the Br-substituted ligand, this has already been confirmed experimentally.[11]

2.2.2. hipt_p. Substitution of the *amine* nitrogen atom by phosphorus leads to [(HIPTN$_3$P)Mo] (**hipt_p**) complexes (see also Supporting Information, Figure S2). Because the ligand is modified at the *trans* position much closer to the central molybdenum than in the previous two cases, one would expect greater changes in the reaction energies (*trans* effect). Table 3 shows that this is the case indeed; the energy differences amount to ± 60 kJ mol^{-1} (depending on the particular reaction step).

To ensure that the differences between the **hipt_p** and **hipt** system are not blurred by conformational effects, we took a closer look at the reaction leading from [**Mo**](N) to [**Mo**](NH) for which the largest difference in reaction energy is obtained. From an overlay of the [**Mo**](N) and [**Mo**](NH) complexes for both ligands (see Supporting Information, Figure S3), one can see that the change in the structure upon protonation of the nitride moiety is larger for **hipt** than for **hipt_p**. However, the changes for **hipt** are still so small that the conformation of the ligand is conserved.

The geometry change for the [(**hipt**)Mo](NH) complex is similar to that of the [(**hipt**)Mo](N)$^+$ fragment[3] obtained after dissociation of ammonia from [(**hipt**)]Mo(NNH$_3$)$^+$ (see also Supporting Information, Figure S4). The latter change in

Table 4. Selected Bond Lengths (Å) for Some Complexes[a]

	hipt		hipt_p		tpa_me		timen(3)	
	$Mo-N^{\alpha}$	$N^{\alpha}-N^{\beta}$	$Mo-N^{\alpha}$	$N^{\alpha}-N^{\beta}$	$Mo-N^{\alpha}$	$N^{\alpha}-N^{\beta}$	$Mo-N^{\alpha}$	$N^{\alpha}-N^{\beta}$
[**Mo**](N_2)	1.984	1.142	2.059	1.135	2.000	1.135	2.016	1.126
[**Mo**](NNH)	1.810	1.237	1.848	1.231	1.817	1.223	1.828	1.196
[**Mo**](NNH_2)	1.847	1.322	1.851	1.307	1.794	1.307	1.771	1.278
[**Mo**](N)	1.680		1.701		1.678		1.670	
[**Mo**](NH)	1.801		1.796		1.754		1.724	
[**Mo**](NH_2)	1.949		1.996		1.933		1.899	
[**Mo**](NH_3)	2.288		2.369		2.271		2.210	

[a] For comparison, the N−N distance in free N_2 is calculated to be 1.104 Å.

Table 5. Complexation Energies (kJ mol^{-1}) of N_2 and NH_3 in the Corresponding [**Mo**](N_2) and [**Mo**](NH_3) Complexes[a]

	N_2	NH_3
hipt	−151.8	−111.3
hipt_oh	−158.2	−107.3
hipt_br	−154.6	−112.0
hipt_p	−91.4	−87.0
htbt	−141.2	−109.0
tpa_me	−134.7	−139.5
tpa_et	−105.6	−142.8
timen(3)	−97.2	−176.6
timen(0)	−193.9	−82.5

[a] The difference between these two energies is identical to the reaction energy for the NH_3/N_2 exchange. Note that these values have not been corrected for basis set superposition effects as these are likely to be 10 kJ mol^{-1} or less (see, for instance, ref 26).

geometry is known to correspond to a change in energy of about 60 kJ mol^{-1}.[3] To obtain similar data for the protonation of the nitride moiety, we deleted the additional hydrogen atom in the [**Mo**](NH) complexes and reoptimized the wave function for both complexes. From these single-point calculations, the energy change associated with structural changes upon protonation of the nitride can be estimated. For the **hipt** ligand, we obtained 43.1 kJ mol^{-1} and for **hipt_p** 48.9 kJ mol^{-1}. The difference between both values is 5.8 kJ mol^{-1} and, thus, the contribution of the relaxation of the ligand to the reaction energy is comparable for both **hipt** and **hipt_p**. Therefore, the calculated difference in reaction energies when comparing **hipt** and **hipt_p** (61 kJ mol^{-1}) cannot be solely because of conformational effects. In fact, the latter contribute only approximately 10% to the overall reaction energy difference.

The introduction of the phosphorus atom is quite beneficial for the thermodynamics of the overall catalytic cycle (see Table 2). For the two thermodynamically most difficult steps with **hipt**, that is, transfer of the second and fourth electron/proton pair, the reaction becomes more exothermic by 15 and 60 kJ mol^{-1}, respectively. On the other hand, formation of the first molecule of ammonia becomes more endothermic by 60 kJ mol^{-1}. However, this does not impose any difficulties since this step still remains the most exothermic one. The NH_3/N_2 exchange is thermodynamically essentially neutral (Table 1).

The $N^{\alpha}-N^{\beta}$ bond lengths are found to be somewhat shorter (Table 4) for **hipt_p**. The Mo−N bond distances are generally longer than for **hipt** (see also Supporting Information, Figures S1 and S2) indicative of a weaker binding of the substrate. Table 5 shows that the bonding energy of N_2 in [(**hipt_p**)Mo](N_2) is 66.9 kJ mol^{-1} smaller than in [(**hipt**)Mo](N_2). Similarly, NH_3 is less bound by 30.8 kJ mol^{-1} in [(**hipt_p**)Mo](NH_3). Since for **hipt_p** the binding of N_2 is more weakened than for NH_3, the NH_3/N_2 exchange becomes less favorable as mentioned above.

2.2.3. htbt. By replacing the *iso*-propyl groups in the terphenyl moieties of [$HIPTN_3NMo$] (**hipt**) by the bulkier *tert*-butyl groups one arrives at the [$HTBTN_3NMo$] complex (**htbt**, Figure 1). Table 3 shows that the reaction energies are comparable to that of **hipt**. The differences are no larger than 8 kJ mol^{-1} and thus comparable to **hipt_oh** and **hipt_br**. From a *thermodynamic* point of view, **htbt** should be as good a ligand for catalysis as **hipt**. However, because of the *tert*-butyl groups, the reaction center is much more crowded and protonation should occur much more slowly because lutidinium may have difficulties entering the reaction cavity at the Mo center.[3]

Experimentally, complexes with **htbt** were found to be barely catalytically active (no more than 10% yield of NH_3).[11] The low activity was appointed to a combination of problems with the reduction of [(**htbt**)Mo]$(NH_3)^+$ and a supposed slowdown of all steps because of overall crowding.[11] Our calculations show that reduction of [(**htbt**)-Mo]$(NH_3)^+$ requires an energy which is only 10 kJ mol^{-1} larger than that of [(**hipt**)Mo]$(NH_3)^+$. This is in agreement with the fact that [(**htbt**)Mo]$(NH_3)^+$ is reduced at a potential 100 mV more negative than [(**hipt**)Mo]$(NH_3)^+$.[11]

2.2.4. tpa_me and tpa_et. Aryl substituted tris(pyrrolyl-α-methyl)amine molybdenum complexes have been suggested by Schrock et al. as potential catalysts for dinitrogen reduction.[13] However, their catalytic activity has not been assessed yet. We therefore also provide data for complexes with the 2,4,6-iso-propyl phenyl substituted ligand (**tpa_me**). Table 3 shows that this ligand is even better than the **hipt_p** ligand. Transfer of the second and fourth electron/proton pair is further facilitated. For the third and fifth pair the energy rises but the overall reaction remains exothermic with the usually applied metallocenes.[3] Problems may arise with the very last step, the NH_3/N_2 exchange, which is calculated to be slightly endothermic (5 kJ mol^{-1}) but which can, however, be regarded as essentially thermoneutral within the accuracy of the applied DFT method. The slight endothermicity is caused by an increased bond energy for NH_3 (139.5 kJ mol^{-1}) in conjunction with a reduced one for N_2 (134.7 kJ mol^{-1}). This can also clearly be seen from the bond lengths in Table 4; for [**Mo**](N_2), the $Mo-N^{\alpha}$ bond is longer for **tpa_me** while it is shorter by the same amount for [**Mo**](NH_3). The lengths of the N(pyrrole)−Mo bonds (Figure 2) are larger than the corresponding bonds in the **hipt** complexes.

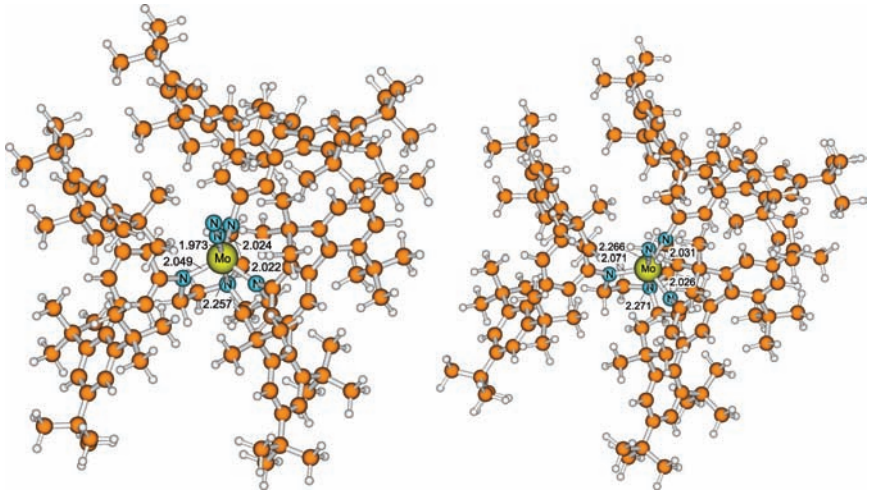

Figure 1. Optimized structures of the [(**htbt**)Mo](N$_2$) (left) and [(**htbt**)Mo](NH$_3$) complex (right). Bond lengths are given in angstrom.

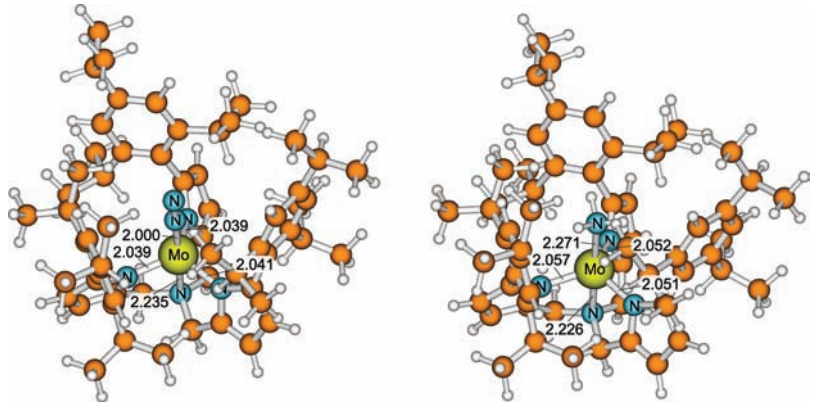

Figure 2. Optimized structures of the [(**tpa_me**)Mo](N$_2$) (left) and [(**tpa_me**)Mo](NH$_3$) complex (right). Bond lengths are given in angstrom.

Extension of the linker between the amine nitrogen atom and the pyrrole moieties by an additional methylene group leads to tris(pyrrolyl-α-ethyl)amine complexes, **tpa_et**. Table 2 shows that in comparison to **tpa_me**, some steps become more and others less favorable but all remain exothermic under the usually applied reaction conditions. The NH$_3$/N$_2$ exchange reaction, however, is quite endothermic (+37.3 kJ mol^{-1}). Interestingly, this increased endothermicity is almost entirely caused by a reduced binding energy of N$_2$ while that of NH$_3$ changes only slightly (see Table 5). Because of the rather unfeasible NH$_3$/N$_2$ exchange, we do not expect complexes with the **tpa_et** ligand to be successful catalysts for dinitrogen reduction.

2.2.5. timen. Alkylidene ligands are known to stabilize high oxidation states of the coordinated metal,[27] and corresponding molybdenum complexes are well-known in the context of metathesis.[28−30] *N*-heterocyclic carbenes are especially suited for catalytic cycles involving reduction and/or oxidation because they are able to stabilize a broad range of oxidation states.[31] Various tris[2-(3-aryl-imidazol-2-ylidene)ethyl]amine (TIMEN^{R}) ligands[14,32] were recently applied in the synthesis of iron nitride complexes as models of nitrogenase.[33]

We therefore decided to explore the potential of molybdenum TIMEN^{R} complexes for catalytic reduction of dinitrogen. In contrast to all other ligands investigated in the present study, the central molybdenum in the resulting complexes is not coordinated by at least three nitrogen donor atoms but rather by three carbon atoms and only one nitrogen atom (see Figure 3). It is reasonable to assume that in the intermediate nitrido species,[34,35] molybdenum has the same formal oxidation state +VI as in [(**hipt**)Mo](N). Because the TIMEN^{R} ligands are neutral, the resulting molybdenum complexes must therefore bear a positive charge of +3.

As potential catalyst we choose the [(TIMEN^{xyl})Mo]$^{3+}$ system, **timen(3)**. The data in Table 2 show that all reduction/protonation steps are exothermic under the commonly applied

(26) Reiher, M.; Hess, B. A. *Chem.—Eur. J.* **2002**, *8*, 5332–5339.
(27) Schrock, R. R. *Chem. Rev.* **2002**, *102*, 145–180.
(28) Chauvin, Y. *Angew. Chem., Int. Ed.* **2006**, *45*, 3740–3747; *Angew. Chem.* **2006**, *118*, 3824−3831.
(29) Schrock, R. R. *Angew. Chem., Int. Ed.* **2006**, *45*, 3748–3759; *Angew. Chem.* **2006**, *118*, 3832−3844.
(30) Grubbs, R. H. *Angew. Chem., Int. Ed.* **2006**, *45*, 3760–3765; *Angew. Chem.* **2006**, *118*, 3845−3850.
(31) Herrmann, W. A.; Köcher, C. *Angew. Chem., Int. Ed.* **1997**, *36*, 2162–2187; *Angew. Chem.* **1997**, *109*, 2256−2282.
(32) Meyer, K.; Bart, S. C. *Adv. Inorg. Chem.* **2008**, *60*, 1–30.
(33) Vogel, C.; Heinemann, F. W.; Sutter, J.; Anthon, C.; Meyer, K. *Angew. Chem., Int. Ed.* **2008**, *47*, 2681–2684; *Angew. Chem.* **2008**, *120*, 2721−2724.
(34) Dehnicke, K.; Strähle, J. *Angew. Chem., Int. Ed.* **1981**, *20*, 413–426; *Angew. Chem.* **1981**, *93*, 451−464.
(35) Dehnicke, K.; Strähle, J. *Angew. Chem., Int. Ed.* **1992**, *31*, 955–978; *Angew. Chem.* **1992**, *104*, 978−1000.

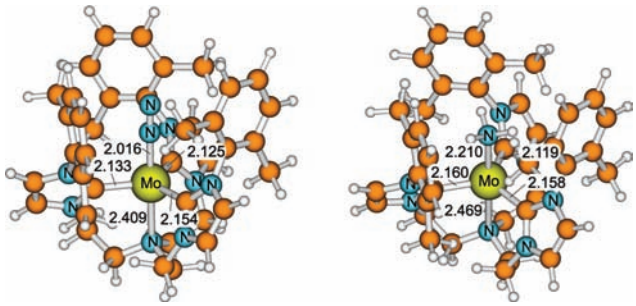

Figure 3. Optimized structures of the [(**timen**)Mo](N$_2$)$^{3+}$ (left) and [(**timen**)Mo](NH$_3$)$^{3+}$ complex (right). Bond lengths are given in angstrom.

reaction conditions, that is, with lutidinium and Cr(cp*)$_2$. Furthermore, the second and fourth step, which are almost thermodynamically neutral for the **hipt** ligand, are exothermic by more than 100 kJ mol^{-1} (see also Table 3). Thus, we predict [(**timen**)Mo]$^{3+}$ to highly facilitate the reduction of dinitrogen in comparison to [(**hipt**)Mo].

However, this will very likely be limited to *stoichiometric* reactions. The replacement of NH$_3$ by N$_2$ required to close the catalytic cycle is calculated to be endothermic by approximately 80 kJ mol^{-1}. This is more than twice the value of 36.4 kJ mol^{-1} calculated for the NH$_3$/N$_2$ exchange reaction of [(**hipt**)Mo](NH$_3$)$^+$.[4] Schrock et al. found the latter reaction to be experimentally unfavorable and emphasized that an efficient NH$_3$/N$_2$ exchange is imperative for catalysis.[36] Therefore, it is rather unlikely that the [(**timen**)Mo]$^{3+}$ system will prove to be a successful catalyst.

The reason for the pronounced endothermicity of the exchange reaction is on the one hand a stronger binding of NH$_3$ in [(**timen**)Mo](NH$_3$)$^{3+}$ by 65.3 kJ mol^{-1} as compared to [(**hipt**)Mo](NH$_3$), see Table 5. On the other hand, N$_2$ is bound weaker by 54.6 kJ mol^{-1} in the corresponding complex. In summary, both effects result in an increase of 119.9 kJ mol^{-1} for the exchange reaction energy (Table 3). This is also reflected in the Mo−N$^\alpha$ bond lengths (Table 4): With the **timen** ligand, for [**Mo**](N$_2$) the bond length increases while it decreases for [**Mo**](NH$_3$).

Spin states of higher multiplicity have been found to play only a minor role for complexes with the **hipt** ligand,[3] and the same behavior can be expected for all the ligands derived from **hipt** (see also below). For the **timen(3)** complexes, however, this assumption may not be valid. Therefore, we calculated the vertical energy splitting between the state of lowest and second lowest multiplicity for the important intermediates (see Computational Details). Table 6 shows that with the exception of the [(**timen**)Mo](NH$_2$)$^{3+}$ and [(**timen**)Mo](NH$_3$)$^{3+}$ complexes, the spin state with lowest multiplicity is also the ground state. For the latter two, the states with $S = 1$ and $S = 1.5$, respectively, are found to be the ground states. Therefore, the [(**timen**)Mo](NH$_3$)$^{3+}$ complex is further stabilized with respect to [(**timen**)Mo](N$_2$)$^{3+}$ and, hence, the exchange reaction becomes even more unfeasible. Thus, the conclusions drawn above are retained even if different spin states are accounted for.

(36) Yandulov, D. V.; Schrock, R. R. *Inorg. Chem.* **2005**, *44*, 1103–1117.

Table 6. Energy Splitting (kJ mol^{-1}) between the Spin State of Lowest and Second Lowest Multiplicity As Obtained from B3LYP* Single-Point Calculations on the BP86 Optimal Structure of the Spin State with Lowest Multiplicity

	timen(3)	**timen(0)**
[**Mo**](N$_2$)	+62.0	+59.2
[**Mo**](NNH)	+91.6	+155.5
[**Mo**](NNH$_2$)	+170.5	+130.9
[**Mo**](N)	+132.5	+175.7
[**Mo**](NH)	+162.7	+145.8
[**Mo**](NH$_2$)	−19.0	+88.7
[**Mo**](NH$_3$)	−5.9	+20.4

From a thermodynamical point of view, the major problem of the **timen(3)** system preventing its potential use as a catalyst for dinitrogen reduction is the energetically unfeasible NH$_3$/N$_2$ exchange reaction. To improve on this situation, it seems desirable to increase the binding energy of dinitrogen while, ideally, that of ammonia decreases simultaneously. If these effects are strong enough, the exchange reaction may become finally exothermic and, thus, catalysis should be feasible. N$_2$ is a σ-donor π-acceptor ligand, and the isoelectronic CO is known to stabilize metals in low oxidation states because of its π-acceptor capabilities.[37,38] Therefore, an obvious approach would be to reduce the formal oxidation state of the central molybdenum atom because reduction of [(**timen**)Mo](N$_2$)$^{3+}$ can be expected to lead to stronger binding of N$_2$ because of enhanced back-bonding from the metal. Ammonia, on the other hand, lacks π-acceptor capabilities and, thus, should be bound more weakly upon reduction of [(**timen**)Mo](NH$_3$)$^{3+}$.

To verify this hypothesis, we also investigated the [(TIMEN^{xyl})Mo]$^{\pm 0}$ system, **timen(0)**. Table 2 shows that the reduction of the metal has a tremendous effect on the reaction energies; the changes are sometimes larger than 100 kJ mol^{-1} as compared to **timen(3)**. However, very importantly, all protonation/reduction steps remain exothermic under the usually applied reaction conditions. The perhaps most striking feature is that, as intended, the NH$_3$/N$_2$ exchange reaction becomes exothermic by −111.4 kJ mol^{-1} (see Table 2). This is almost three times the value for **hipt** and, with respect to **timen(3)**, a change by almost 200 kJ mol^{-1}!

Table 5 shows that in [(**timen**)Mo](N$_2$), dinitrogen is bound more strongly by almost 100 kJ mol^{-1} as compared to [(**timen**)Mo](N$_2$)$^{3+}$ while it is vice versa for ammonia. NBO second order perturbation analysis (see Computational Details) indicates that $n_{Mo} \rightarrow \pi^*_{N\equiv N}$ backbonding increases strongly upon reduction. In [(**timen**)Mo](N$_2$), it accounts for a stabilization of about 400 kJ mol^{-1} while it is only 160 kJ mol^{-1} in [(**timen**)Mo](N$_2$)$^{3+}$ or [(**hipt**)Mo](N$_2$).

The spin state with lowest multiplicity is found to be the ground-state for all **timen(0)** complexes, see Table 6. As has been shown in our previous paper, a reoptimization of the geometry in the corresponding spin state employing the B3LYP* functional leads to a decrease in the energy splitting, that is, stabilization of the spin state with higher multiplicity.[3] However, the energy change is usually too small to alter the

(37) Holleman, A. F.; Wiberg, E.; Wiberg, N. *Lehrbuch der Anorganischen Chemie*, 101st ed.; de Gruyter: Berlin, 1995; Chapter 20, p 1246.
(38) Elschenbroich, C.; Salzer, A. *Organometallics*, 2nd ed.; VCH: Weinheim, Germany, 1992; Chapter 14, pp 220−238.

ordering of the spin states; for the **hipt** complexes, the qualitative picture remains unchanged if the splitting is at least +50kJ mol^{-1}.[3] Even if for the [**Mo**](NH_3) complex the state with $S = 1$ were the ground state, this would not have a significant influence on the reaction energies obtained. Formation of [**Mo**](NH_3) would be somewhat more exothermic while the exchange reaction would become a little less exothermic, but these changes will not affect the qualitative picture and thus the conclusions drawn.

To substantiate this rather qualitative argumentation, we also reoptimized the geometry of the [**Mo**](N_2) and [**Mo**](NH_3) complexes for **timen(3)** and **timen(0)** in both spin states employing the B3LYP* functional. As expected, for [**Mo**](N_2) the energy splitting decreases to +13.9 kJ mol^{-1} for **timen(3)** and +17.4 kJ mol^{-1} for **timen(0)**, respectively. Thus, for [**Mo**](N_2) the spin state with lowest multiplicity remains the ground state. Similarly, for the [**Mo**](NH_3) complexes, we obtained values of −32.2 kJ mol^{-1} for **timen(3)** and −14.7 kJ mol^{-1} for **timen(0)**. However, as already argued above, the resulting changes in the reaction energies are too small to alter the qualitative picture.

2.3. Which Parameters Characterize an Efficient Catalyst? Besides its stability under the applied reaction conditions, a successful catalyst must fulfill two requirements: First, all reduction/protonation steps must be feasible and, second, the NH_3/N_2 exchange must also be feasible. As Table 2 shows, the first requirement is easily met by all systems investigated in the present study. The second requirement, however, is much more difficult to accomplish. Albeit all reduction/protonation steps that are potentially difficult with the various HIPT based ligands become significantly more exothermic with the **tpa** or **timen(3)** ligands, this comes at the cost of an unfavorable replacement of ammonia by dinitrogen. Therefore, the success of a particular complex as catalyst is largely determined by the feasibility of the NH_3/N_2 exchange reaction, and we will thus focus on this step in more detail for the remainder of this section.

As has been shown above and in our previous paper,[3] spin states with higher multiplicity may play a role. With the exception of the **timen(0)** system, both [**Mo**](N_2) and [**Mo**](NH_3) are formally Mo(III) complexes in a trigonal bipyramidal environment. From ligand field theory, one would therefore expect a $S = 0.5$ ground-state for Mo(III).[39] Table 7 shows that for all ligands the difference between doublet and quartet states (singlet and triplet states for **timen(0)**) in [**Mo**](N_2) is at least 60 kJ mol^{-1}. Therefore, the spin state with lowest multiplicity is the ground-state for the dinitrogen complexes which for [(**hipt**)Mo](N_2) is also in accord with experimental data.[40] For the ammonia complexes, the energy splittings are generally lower. Similarly to the above discussion of the **timen** system, even if the state with $S = 1.5$ were the ground state, this would only have a minor influence on the reaction energies, and the conclusions drawn are still the same.

Table 7. Energy Splittings (kJ mol^{-1}) between the Two Lowest Spin States of [**Mo**](N_2) and [**Mo**](NH_3) Complexes As Obtained from B3LYP* Single-Point Calculations on the BP86 Optimal Geometry of the Spin State with Lowest Multiplicity

ligand	ΔE (N_2)	ΔE (NH_3)
hipt	+182.1	+99.3
hipt_oh	+185.6	+107.0
hipt_br	+174.4	+94.1
hipt_p	+172.5	+129.1
htbt	+172.2	+88.5
tpa_me	+113.5	+45.4
tpa_et	+110.0	+29.3
timen(3)	+62.0	−5.9
timen(0)	+59.2	+20.4

Reaction energies for the NH_3/N_2 exchange reaction obtained with various computational methods are shown in Table 8. In comparison to the BP86 values, with the B3LYP* functional, reaction energies are systematically more endothermic by approximately 25 kJ mol^{-1}. Therefore, we shall investigate a couple of more functionals to consolidate the energies for this decisive reaction step.

First of all, neither BP86 nor B3LYP* take weak dispersion forces into account. So far, we have assumed that their effect on energies drops out as soon as reaction energies are calculated from the total energies of products and educts. However, we shall test this assumption with a functional that proved to be quite accurate for dispersion dominated systems,[41] namely B97-D. The B97-D data differ by no more than a few kJ mol^{-1} from the BP86 data for all complexes; consequently, corrections due to dispersion are negligible for this reaction. Similarly, solvent effects incorporated by means of the COSMO model (see Computational Details) decrease the reaction energies only by approximately 10 kJ mol^{-1} and, thus, can safely be neglected.

Finally, we calculated reaction energies with the recently proposed M06 density functional. This functional has been shown to perform better than a wide variety of other popular functionals in terms of average errors.[42] Indeed, for the exchange reaction with the **hipt** ligand, the calculated M06//BP86 value (+12.9 kJ mol^{-1}) shows the smallest deviation from experiment[43] (+5.7 kJ mol^{-1}) among all functionals tested. Note, that we assume to good approximation that the electronic energy at 0 K resembles the Gibbs free energy because entropic effects can be neglected for ligand exchange reactions while temperature effects would only modulate the energy differences to a small extent (this assertion is to be understood in view of the general accuracy of DFT calculations). Despite the fact that the absolute reaction energies may differ depending on the density functional, the differences are systematic and similar for all investigated complexes. Thus, the qualitative results are the same for all density functionals under consideration and none of the previous conclusions concerning the suitability of a particular

(39) Holleman, A. F.; Wiberg, E.; Wiberg, N. *Lehrbuch der Anorganischen Chemie*, 101st ed.; de Gruyter: Berlin, 1995; Chapter 20, pp 1250−1270.
(40) McNaughton, R. L.; Chin, J. M.; Weare, W. W.; Schrock, R. R.; Hoffman, B. M. *J. Am. Chem. Soc.* **2007**, *129*, 3480–3481.
(41) Grimme, S. *J. Comput. Chem.* **2006**, *27*, 1787–1799.
(42) Zhao, Y.; Truhlar, D. G. *Acc. Chem. Res.* **2008**, *41*, 157–167.
(43) Weare, W. W.; Dai, X.; Byrnes, M. J.; Chin, J. M.; Schrock, R. R.; Müller, P. *Proc. Natl. Acad. Sci. U.S.A.* **2006**, *103*, 17099–17106.

Table 8. Reaction Energies (kJ mol^{-1}) for the NH_3/N_2 Exchange Reaction Obtained with Different Computational Approaches[a]

ligand	BP86	B3LYP*// BP86	B97-D// BP86	B97-D	COSMO-BP86// BP86	COSMO-BP86	M06//BP86
hipt	−40.5	−13.3	−34.5	−39.0	−47.8	−46.5	+12.9
hipt_oh	−50.9	−22.4	−50.3	−52.8	−60.9	−63.7	−7.4
hipt_br	−42.6	−15.6	−43.1	−40.1	−53.9	−52.4	+5.8
hipt_p	−4.5	+17.4	−3.1	−7.3	−15.0	−15.7	+32.4
htbt	−32.2	−5.4	−31.1	−32.7	−42.8	−46.0	+18.3
tpa_me	+4.9	+32.1	+4.6	+5.8	−4.6	−4.6	+65.0
tpa_et	+37.3	+62.6	+36.9	+37.4	+27.3	+27.3	+87.2
timen(3)	+79.4	+91.9	+77.6	+78.9	+64.4	+64.7	+103.1
timen(0)	−111.4	−107.2	−117.7	−116.8	−127.5	−127.5	−84.0

[a] If the energy was calculated with one electronic structure method for a structure optimized with another method, the double-slash notation is employed. Hence, no double-slash indicates that energy and structure have been obtained with the same method.

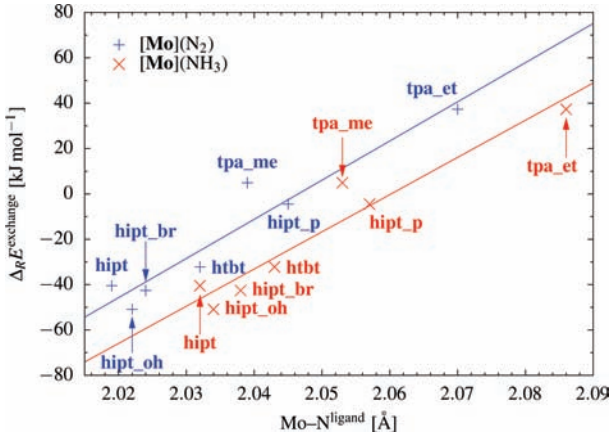

Figure 4. Reaction energy for the NH_3/N_2 exchange versus the average distance between the central molybdenum atom and the equatorial nitrogen atoms in the [**Mo**](N_2) and [**Mo**](NH_3) complexes. The lines correspond to a linear fit, $y = ax + b$. [**Mo**](N_2) complexes: $a = 1730$ kJ mol^{-1} Å^{-1} and $b = -3550$ kJ mol^{-1}. The standard error of a is $\sigma_a = 240$ kJ mol^{-1} Å^{-1} (13.6%) while that of b is $\sigma_b = 480$ kJ mol^{-1} (13.5%). The correlation coefficient is 0.95. [**Mo**](NH_3) complexes: $a = 1640$ kJ mol^{-1} Å^{-1} and $b = -3380$ kJ mol^{-1}. The standard error of a is $\sigma_a = 210$ kJ mol^{-1} Å^{-1} (12.6%) while that of b is $\sigma_b = 430$ kJ mol^{-1} (12.6%). The correlation coefficient is 0.95.

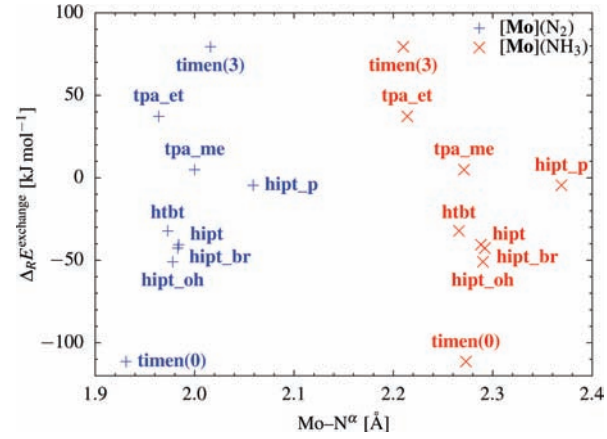

Figure 5. Reaction energy for the NH_3/N_2 exchange versus the distance between the central molybdenum atom and the N^α atom in the [**Mo**](N_2) and [**Mo**](NH_3) complexes.

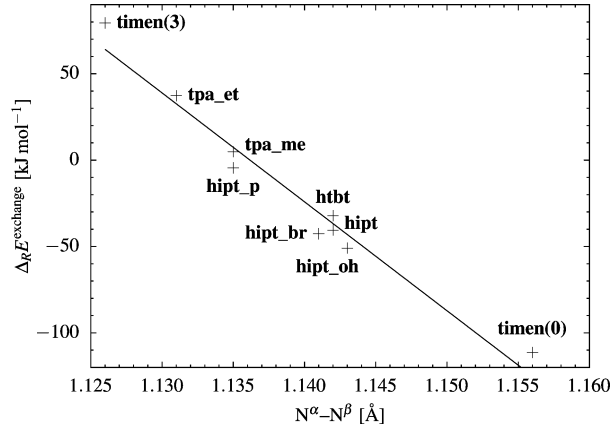

Figure 6. Reaction energy for the NH_3/N_2 exchange versus the distance between the N^α and N^β atoms in [**Mo**](N_2). The line corresponds to a linear fit, $y = ax + b$, with $a = -6310$ kJ mol^{-1} Å^{-1} and $b = 7160$ kJ mol^{-1}. The standard deviation of a is $\sigma_a = 450$ kJ mol^{-1} Å^{-1} (7.1%) while that of b is $\sigma_b = 510$ kJ mol^{-1} (7.1%). The correlation coefficient is 0.98.

complex as potential catalyst are changed. We may therefore continue our discussion based solely on the BP86 data. An advantage of this approach is the fact that calculations employing the latter density functional are computational much more feasible than those with M06 which allows for faster screening of potential catalysts.

Figure 4 shows plots of the exchange reaction energy versus the average bond length between the central molybdenum atom and the three equatorial amide nitrogen atoms in the various [**Mo**](N_2) and [**Mo**](NH_3) complexes, respectively. A good correlation is obtained and the average Mo−N^{ligand} distance can thus serve as a first indicator with shorter Mo−N distances corresponding to smaller (more negative) reaction energies. However, a major drawback of this parameter is that it is limited to ligands where nitrogen coordinates the molybdenum in the equatorial positions. Obviously, this linear structure−reactivity relationship is not applicable to, for example, the **timen** ligand or complexes with phosphorus donor atoms.

A similar plot is shown in Figure 5 for the dependence of the exchange reaction energy on the Mo−N^α bond distance in the [**Mo**](N_2) and [**Mo**](NH_3) complexes, respectively. One immediately sees that no useful correlation between these two quantities exists. Therefore, the Mo−N^α distance cannot serve as an indicator as to whether the exchange reaction will be feasible for a particular ligand.

The most useful indicator is the N^α−N^β bond length (Figure 6) which shows an excellent correlation with the exchange reaction energy (the correlation coefficient is 0.98). The differences in the binding strength of N_2 are predominantly governed by the π back-bonding interaction from the molybdenum (see also discussion of **timen**). Thus, the more strongly N_2 is bound, the longer becomes N^α−N^β because of population of the $\pi^*_{N\equiv N}$ orbitals. Ammonia which lacks these π-acceptor capabilities will therefore coordinate more

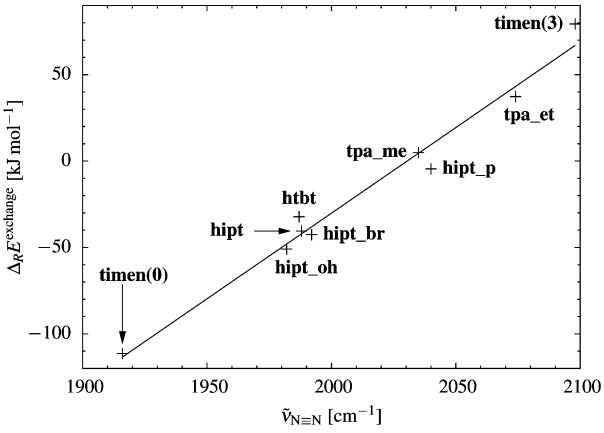

Figure 7. Reaction energy for the NH_3/N_2 exchange versus wavenumber of the N≡N stretching vibration in [**Mo**](N_2). The line corresponds to a linear fit, $y = ax + b$, with $a = 0.991$ kJ mol^{-1} cm and $b = -2010$ kJ mol^{-1}. The standard deviation of a is $\sigma_a = 0.056$ kJ mol^{-1} cm (5.7%) while that of b is $\sigma_b = 110$ kJ mol^{-1} (5.6%). The correlation coefficient is 0.99.

weakly in such complexes. Using the results from the linear fit (see Figure 6), the exchange reaction becomes exothermic for $N^{\alpha}-N^{\beta}$ distances larger than 1.136 Å. Hence, whenever the $N^{\alpha}-N^{\beta}$ bond length is larger than approximately 1.14 Å, one can assume that exchange of ammonia by dinitrogen is feasible. This corresponds to a bond elongation of at least 3.5 pm in comparison to the N−N distance in free N_2 which is calculated to be 1.104 Å.

The feasibility of the exchange reaction can thus already be estimated from the structure of the [**Mo**](N_2) complex. Generally, this information could be obtained with computational methods. However, then it should also not be a problem to perform a similar calculation for the corresponding [**Mo**](NH_3) complex to obtain the exchange reaction energy directly. A much more interesting application is therefore the assessment of the reaction energy directly from the experimentally determined structure of the [**Mo**](N_2) complex. Usually, this would imply the growth of crystals subsequently subjected to X-ray crystallographic analysis. But, in view of the rather small overall change in N≡N bond lengths of only about 0.03 Å (see Figure 6), it is questionable whether the experimental bond lengths thus obtained are accurate to be significant.

As an alternative approach, the strength of the N≡N bond can also be assessed experimentally from the wavenumber of the N≡N stretching mode.[44] In addition, vibrational spectroscopy yields accurate data that can even be obtained directly from the reaction mixture. Figure 7 shows that a strong correlation between the calculated wavenumber $\tilde{\nu}_{N\equiv N}$ and the reaction energy for the NH_3/N_2 exchange exists. For [(**hipt**)Mo](N_2), our calculated value of 1988 cm^{-1} agrees very well with the experimental value[43] of 1990 cm^{-1}. For **htbt**, the same value as for **hipt** was measured,[11] which also agrees well with our calculated value of 1987 cm^{-1}. For **hipt_br**, experiment[11] and calculation yield the same value of 1992 cm^{-1}. Therefore, whenever the wavenumber of the N≡N stretching mode is found to be smaller than 2000 cm^{-1}, the NH_3/N_2 exchange reaction should be thermodynamically feasible.

(44) Himmel, H.-J.; Reiher, M. *Angew. Chem., Int. Ed.* **2006**, *45*, 6264–6288; *Angew. Chem.* **2006**, *118*, 6412−6437.

3. Conclusions

We have investigated several modifications of the [(**hipt**)-Mo] complex as to whether they are potential catalysts for the reduction of dinitrogen to ammonia. Substitution at the *para* position of the central ring in the terphenyl moieties results only in small differences in the reaction energies, and such complexes should therefore show a catalytic activity comparable to that of the parent **hipt** system. In addition, several other ligands were tested. The main problem for a successful catalysis appears to be an efficient exchange of NH_3 by N_2 to both close the catalytic cycle and regenerate the active catalyst. Focusing on this very reaction step, we identified the **timen(0)** system to be the most promising candidate to be tested experimentally. However, while this ligand seems optimal from a thermodynamic point of view, unexpected side reactions may still prevent such complexes from being successful catalysts.

Finally, we derived a structure−reactivity relationship which allows for a convenient estimation of whether the NH_3/N_2 exchange is feasible for a particular complex. To this end, the exchange reaction energy can be estimated simply from the N≡N bond distance with help of the linear function fitted to the data in Figure 6. However, since structural data from experiment might not be accurate enough to resolve small changes in the N≡N bond length, we also included a discussion of the N≡N stretching vibration which can be determined experimentally with sufficient accuracy. It turned out that whenever $\tilde{\nu}_{N\equiv N}$ is found below 2000 cm^{-1}, the NH_3/N_2 exchange reaction should be thermodynamically feasible.

Acknowledgment. The authors thank the Schweizer Nationalfonds SNF (Project no. 200020-121870) for financial support.

Supporting Information Available: Cartesian coordinates of all calculated molecules and additional illustrations. This material is available free of charge via the Internet at http://pubs.acs.org.

Appendix

Computational Details

All energy calculations and structure optimizations were carried out with the density functional programs provided by the Turbomole 5.7 suite.[45] Our previous results[3] indicate that kinetics does not play a dominant role and that the mechanism may be studied by considering thermodynamics only. For all closed-shell electronic structures we employed a restricted framework, while we switched to unrestricted Kohn−Sham calculations for the open-shell complexes. We used the Becke−Perdew exchange−correlation functional dubbed BP86[46,47] as implemented in Turbomole. Although it has been noted that reaction energies for dinitrogen activation may vary substantially with the choice of density

functional,[48] we have demonstrated in our previous work[5] that for the complexes under investigation the differences between the hybrid B3LYP[49] and the BP86 functional are usually negligible in view of the general accuracy of DFT calculations. We therefore applied only the pure BP86 functional, for which we can invoke the efficient density-fitting resolution-of-the-identity (RI) techniques available in Turbomole.

For molybdenum and hetero atoms, we used Ahlrichs' valence triple-ζ TZVP basis set with polarization functions.[50] For the carbon and hydrogen atoms, we used the smaller split-valence plus polarization functions (SVP) basis set.[51] For the complexes with the **timen** ligand, the TZVP basis set was also used for the three carbene carbon atoms. The corresponding RI auxiliary basis sets were taken from the Turbomole library. For the molybdenum atom, a Stuttgart−Dresden effective core potential (ECP) was applied.[52] This ECP also guarantees a reasonable modeling of scalar-relativistic effects on molybdenum.

All molecular structures were fully optimized until the length of the gradient vector had approached about 0.001 au and the energetical difference of the last twenty structures in the optimization procedure was below 1 kJ mol^{-1}. The *para* and *tert*-butyl substituted ligands were derived from the structure of [(**hipt**)Mo] reported in ref 3. For the initial optimization of the structure of the [(**tpa_me**)Mo] complex, we used the crystal structure[13] of [(**tpa_me**)MoCl] as starting point. Similarly, the crystal structure[33] of [(**timen**)FeN] was used as starting point for the optimization of [(**timen**)Mo]. The initial structure of the [(**tpa_et**)Mo] complex was derived from that of [(**timen**)Mo]. All further structures were optimized starting from the pre-optimized arrangement for the particular ligand L, [(L)Mo], to reduce conformational effects on the reaction energies to a minimum. If not mentioned otherwise, all optimizations were performed for the spin state with lowest multiplicity. We should emphasize that the complexes under investigation comprise up to 330 atoms which were all treated explicitly (with the exception of the core electrons of the molybdenum that were replaced by the ECP).

For the NH_3/N_2 exchange reaction, solvent effects were estimated within the conductor-like screening model (COSMO).[53−55] As solvent we chose *n*-heptane with $\varepsilon = 1.92$. For H, C, N, O, and Br, the optimized cavity radii 1.30, 2.00, 1.83, 1.72, 2.16 Å, respectively, were used.[56] For Mo and P, no such optimized radii are available and we therefore chose 1.17 times the van der Waals radius[57,58] (2.223 and 2.106 Å, respectively) which is a generally well accepted rule.[56] It has been shown that for different metals (including Mo) the electronic energies are quite insensitive to the particular choice of the cavity radius since the metal is normally buried deep inside the cavity.[59] For all other parameters, the default values of Turbomole were used which includes closing of the solvent accessible surface and an outlying charge correction.[54]

Likewise, corrections due to long-range dispersion were estimated by employing the B97-D density functional which empirically accounts for van der Waals interactions.[41,60] Since this functional is not available in Turbomole 5.7, we used the 5.10 version instead for these calculations.

Single-point calculations with the M06 density functional[42,61] were carried out with the NWChem program.[62,63] This functional has been shown to be more accurate than a great variety of other functionals for certain molecules.[61] For the M06 calculations, the same TZVP-SVP basis set and ECP (for molybdenum) used throughout this study was employed.

Energy splittings between different spin states were obtained by single-point calculations with our B3LYP* functional on the BP86 optimal structure of the spin state with lowest multiplicity. B3LYP* is a B3LYP functional with only 15% exact exchange admixture reparametrized for the energy splitting of states of different spin.[64−66] All B3LYP* calculations including those for $S = 0$ were carried out in an unrestricted framework.

(45) Ahlrichs, R.; Bär, M.; Häser, M.; Horn, H.; Kölmel, C. *Chem. Phys. Lett.* **1989**, *162*, 165–169.
(46) Becke, A. D. *Phys. Rev. A: At., Mol., Opt. Phys.* **1988**, *38*, 3098–3100.
(47) Perdew, J. P. *Phys. Rev. B: Condens. Matter Mater. Phys.* **1986**, *33*, 8822–8824.
(48) Graham, D. C.; Beran, G. J. O.; Head-Gordon, M.; Christian, G.; Stranger, R.; Yates, B. F. *J. Phys. Chem. A* **2005**, *109*, 6762–6772.
(49) Stephens, P. J.; Devlin, F. J.; Chabalowski, C. F.; Frisch, M. J. *J. Phys. Chem.* **1994**, *98*, 11623–11627.
(50) Schäfer, A.; Huber, C.; Ahlrichs, R. *J. Chem. Phys.* **1994**, *100*, 5829–5835.
(51) Schäfer, A.; Horn, H.; Ahlrichs, R. *J. Chem. Phys.* **1992**, *97*, 2571–2577.
(52) Andrae, D.; Häußermann, U.; Dolg, M.; Stoll, H.; Preuß, H. *Theor. Chim. Acta* **1990**, *77*, 123–141.
(53) Klamt, A.; Schüürmann, G. *J. Chem. Soc., Perkin Trans. 2* **1993**, 799–805.
(54) Schäfer, A.; Klamt, A.; Sattel, D.; Lohrenz, J. C. W.; Eckert, F. *Phys. Chem. Chem. Phys.* **2000**, *2*, 2187–2193.
(55) Tomasi, J.; Mennucci, B.; Cammi, R. *Chem. Rev.* **2005**, *105*, 2999–3093.
(56) Klamt, A.; Jonas, V.; Bürger, T.; Lohrenz, J. C. W. *J. Phys. Chem. A* **1998**, *102*, 5074–5085.
(57) Bondi, A. *J. Phys. Chem.* **1964**, *68*, 441–451.
(58) Bondi, A. *J. Phys. Chem.* **1966**, *70*, 3006–3007.
(59) Jensen, K. P. *J. Inorg. Biochem.* **2008**, *102*, 87–100.
(60) Grimme, S. *J. Comput. Chem.* **2004**, *25*, 1463–1473.
(61) Zhao, Y.; Truhlar, D. *Theor. Chem. Acc.* **2008**, *120*, 215–241.
(62) Kendall, R. A.; Aprà, E.; Bernholdt, D. E.; Bylaska, E. J.; Dupuis, M.; Fann, G. I.; Harrison, R. J.; Ju, J.; Nichols, J. A.; Nieplocha, J.; Straatsma, T. P.; Windus, T. L.; Wong, A. T. *Comput. Phys. Commun.* **2000**, *128*, 260–283.
(63) Bylaska, E. J.; de Jong, W. A.; Govind, N.; Kowalski, K.; Straatsma, T. P.; Valiev, M.; Wang, D.; Apra, E.; Windus, T. L.; Hammond, J.; Nichols, P.; Hirata, S.; Hackler, M. T.; Zhao, Y.; Fan, P.-D.; Harrison, R. J.; Dupuis, M.; Smith, D. M. A.; Nieplocha, J.; Tipparaju, V.; Krishnan, M.; Wu, Q.; Van Voorhis, T.; Auer, A. A.; Nooijen, M.; Brown, E.; Cisneros, G.; Fann, G. I.; Fruchtl, H.; Garza, J.; Hirao, K.; Kendall, R.; Nichols, J. A.; Tsemekhman, K.; Wolinski, K.; Anchell, J.; Bernholdt, D.; Borowski, P.; Clark, T.; Clerc, D.; Dachsel, H.; Deegan, M.; Dyall, K.; Elwood, D.; Glendening, E.; Gutowski, M.; Hess, A.; Jaffe, J.; Johnson, B.; Ju, J.; Kobayashi, R.; Kutteh, R.; Lin, Z.; Littlefield, R.; Long, X.; Meng, B.; Nakajima, T.; Niu, S.; Pollack, L.; Rosing, M.; Sandrone, G.; Stave, M.; Taylor, H.; Thomas, G.; van Lenthe, J.; Wong, A.; Zhang, Z. *NWChem, A Computational Chemistry Package for Parallel Computers*, version 5.1; Pacific Northwest National Laboratory: Richland, WA, 2007.
(64) Reiher, M.; Salomon, O.; Hess, B. A. *Theor. Chem. Acc.* **2001**, *107*, 48–55.
(65) Reiher, M. *Inorg. Chem.* **2002**, *41*, 6928–6935.
(66) Salomon, O.; Reiher, M.; Hess, B. A. *J. Chem. Phys.* **2002**, *117*, 4729–4737.

Natural bond orbital analysis[67,68] (NBO) was performed using the NBO-5G program[69] as interfaced to Gaussian03[70] at the BP86 optimal structure using the B3LYP* Kohn−Sham orbitals (B3LYP*//BP86). To avoid an expensive recalculation of the MO coefficients with Gaussian, we reused the converged values obtained from the corresponding Turbomole calculations. To this end, we first transformed the Turbomole data into Molden[71] input format. This file was then converted into Gaussian input. The subsequent Gaussian calculation uses the Turbomole optimized MOs as the initial guess. The basis set (which was also converted) and the ECP for molybdenum are the same as those employed in the Turbomole calculations. Using this protocol, SCF convergence is achieved after one cycle. Note, that the definition of the B3LYP functional slightly differs in both programs. Turbomole uses the (recommended) VWN[72] interpolation form V while Gaussian uses form I.[73] Since B3LYP* is simply the B3LYP functional with reduced exact exchange,[64] this also affects our calculations. Therefore, to employ VWN form V, we used the ubv5lyp iop(3/76=1000001500) iop(3/77=0720008500) iop(3/78=0810010000) keyword combination for Gaussian, which we give here for the sake of reproducibility.

For the seminumerical calculation of vibrational frequencies and normal modes, the mode-tracking vibrational spectroscopy package Akira[74,75] was used which allows one to calculate only selected parts of the vibrational spectrum. Vibrational analysis using mode-tracking has been recently reviewed.[76,77] Wave function convergence was achieved to better than 10^{-8} a.u. in terms of the electronic energy change. All frequencies were used without scaling since previous investigations[78−81] demonstrated the reliability and accuracy of the BP86/TZVP method and yielded a scaling factor of unity.[82]

Molecular structure representations were created with the program Molden.[71]

IC802037W

(67) Weinhold, F.; Landis, C. R. *Valency and Bonding*; Cambridge University Press: Cambridge, U.K., 2005.
(68) Reed, A. E.; Curtiss, L. A.; Weinhold, F. *Chem. Rev.* **1988**, *88*, 899–926.
(69) Weinhold, F. *NBO*, version 5; http://www.chem.wisc.edu/~nbo5/ (accessed Sept 26, 2008).
(70) Frisch, M. J.; Trucks, G. W.; Schlegel, H. B.; Scuseria, G. E.; Robb, M. A.; Cheeseman, J. R.; Montgomery, J. A., Jr.; Vreven, T.; Kudin, K. N.; Burant, J. C.; Millam, J. M.; Iyengar, S. S.; Tomasi, J.; Barone, V.; Mennucci, B.; Cossi, M.; Scalmani, G.; Rega, N.; Petersson, G. A.; Nakatsuji, H.; Hada, M.; Ehara, M.; Toyota, K.; Fukuda, R.; Hasegawa, J.; Ishida, M.; Nakajima, T.; Honda, Y.; Kitao, O.; Nakai, H.; Klene, M.; Li, X.; Knox, J. E.; Hratchian, H. P.; Cross, J. B.; Bakken, V.; Adamo, C.; Jaramillo, J.; Gomperts, R.; Stratmann, R. E.; Yazyev, O.; Austin, A. J.; Cammi, R.; Pomelli, C.; Ochterski, J. W.; Ayala, P. Y.; Morokuma, K.; Voth, G. A.; Salvador, P.; Dannenberg, J. J.; Zakrzewski, V. G.; Dapprich, S.; Daniels, A. D.; Strain, M. C.; Farkas, O.; Malick, D. K.; Rabuck, A. D.; Raghavachari, K.; Foresman, J. B.; Ortiz, J. V.; Cui, Q.; Baboul, A. G.; Clifford, S.; Cioslowski, J.; Stefanov, B. B.; Liu, G.; Liashenko, A.; Piskorz, P.; Komaromi, I.; Martin, R. L.; Fox, D. J.; Keith, T.; Al-Laham, M. A.; Peng, C. Y.; Nanayakkara, A.; Challacombe, M.; Gill, P. M. W.; Johnson, B.; Chen, W.; Wong, M. W.; Gonzalez, C.; Pople, J. A. *Gaussian03*, revision D.01; Gaussian, Inc.: Wallingford, CT, 2004; http://www.gaussian.com (accessed Sept 26, 2008).
(71) Schaftenaar, G.; Noordik, J. H. *J. Comput. Aided Mol. Des.* **2000**, *14*, 123–134; http://www.cmbi.ru.nl/molden/molden.html (accessed Sept 26, 2008). .
(72) Vosko, S. H.; Wilk, L.; Nusair, M. *Can. J. Phys.* **1980**, *58*, 1200–1211.
(73) Scuseria, G. E.; Staroverov, V. N. In *Theory and Applications of Computational Chemistry: The First Forty Years*; Dykstra, C. E.; Frenking, G.; Kim, K. S.; Scuseria, G. E., Eds.; Elsevier: Amsterdam, 2005; Chapter 24, pp 669−724.
(74) Reiher, M.; Neugebauer, J. *J. Chem. Phys.* **2003**, *118*, 1634–1641.
(75) Neugebauer, J.; Herrmann, C.; Reiher, M. *Akira*; http://www.theochem.ethz.ch/software/akira (accessed Sept 26, 2008).
(76) Herrmann, C.; Reiher, M. *Top. Curr. Chem.* **2007**, *268*, 85–132.
(77) Herrmann, C.; Neugebauer, J.; Reiher, M. *New J. Chem.* **2007**, *31*, 818–831.
(78) Brehm, G.; Reiher, M.; Le Guennic, B.; Leibold, M.; Schindler, S.; Heinemann, F. W.; Schneider, S. *J. Raman Spectrosc.* **2006**, *37*, 108–122.
(79) Reiher, M.; Brehm, G.; Schneider, S. *J. Phys. Chem. A* **2004**, *108*, 734–742.
(80) Reiher, M.; Neugebauer, J.; Hess, B. A. *Z. Phys. Chem.* **2003**, *217*, 91–104.
(81) Brehm, G.; Reiher, M.; Schneider, S. *J. Phys. Chem. A* **2002**, *106*, 12024–12034.
(82) Neugebauer, J.; Hess, B. A. *J. Chem. Phys.* **2003**, *118*, 7215–7225.